

# Design of Heterostructures for High Efficiency Thermionic Emission

Zhixi Bian and Ali Shakouri  
Electrical Engineering Department, University of California  
Santa Cruz, CA 95064, U.S.A.

## ABSTRACT

We use two heterostructure designs to improve the energy conversion efficiency of solid-state thermionic devices. The first method is to use a non-planar heterostructure with roughness in order of electron mean free path. This has some combined benefits of increased effective interface area, and reduced total internal reflection for the electron trajectories arriving at the interface. Monte Carlo simulations of various geometries show that the electrical conductivity and thermoelectric figure of merit can be improved for non-planar barrier compared to the planar counterpart. The second method is to use planar high barrier heterostructures with different effective masses for charge carriers in emitter and barrier regions. When an electron passes from a lower effective mass emitter and arrives at a barrier with higher effective mass, since both the lateral momentum and total energy are conserved, part of the lateral energy is coupled to the vertical direction and the electron gains momentum in the direction perpendicular to the interface to enter the barrier region. For high potential barriers, the improvement of thermionic current is about the same as the ratio of the effective masses of the two materials, which can be a factor of 5-10 for typical heterostructure material systems.

## INTRODUCTION

The performance of a thermoelectric device is mostly determined by the dimensionless figure of merit  $ZT$ .  $ZT$  is defined as  $ZT = (S^2 \sigma / k) T$ , where  $T$  is the absolute temperature,  $S$  is the Seebeck coefficient, and  $\sigma$  and  $k$  are the electrical and thermal conductivities, respectively [1]. Solid-state thermionic energy converters are expected to offer a larger thermoelectric power factor ( $S^2 \sigma$ ) than uniform bulk materials due to the selective emission of hot electrons while maintaining a similar electrical conductivity as highly degenerate emitter materials [2, 3]. However, it has been shown that such electronic-transport enhancing technique can only improve the thermoelectric property up to a point [4]. Instead, the advantage of conventional planar superlattices or multilayers is in the reduction of phonon transport and the parasitic heat loss [5, 6]. The main shortcoming of planar barriers is that they only transmit electrons whose kinetic energy in the direction perpendicular to the barrier is large enough. To use the total kinetic energy to overcome the potential barrier, we proposed to use controlled roughness at the heterostructure interfaces to break the in-plane translational invariance and lateral momentum conservation [7]. The nonpitaxial interface scattering and lateral momentum nonconservation have been verified by ballistic electron emission microscopy for some metal/semiconductor interfaces [8, 9]. However, the enhancement of the total thermionic emission current needs to be further quantified for these experiments. In this paper, we introduce two heterostructure designs to increase the thermionic emission current and electrical conductivity: the first method is based on a non-planar barrier; the second one is based on a planar barrier with a larger effective mass compared to the emitter.

## NON-PLANAR BARRIERS

A schematic of the heterostructure thermionic device with the zigzagged interface is shown in Fig. 1 (a). In real space, the effective interface area between the emitter and the barrier is increased for zigzagged structures. However taking into account only the geometrical increased surface area is not sufficient. One has to consider the length scale of the roughness relative to the electron mean-free-path. An electron that crosses the interface may reenter the emitter region in a rough heterostructure even without any scattering. On the other hand, an electron that is reflected from the barrier by total internal reflection may hit the next barrier surface with a smaller angle with respect to normal and thus enter the barrier region in the second try. As it can be seen in Fig. 1(b), more electrons have a chance to pass over the barrier in a triangle region. This phenomenon of directing electron trajectory has an analogy in ray optics for photon extraction in a light emitting diode (LED) die [10].

## SIMULATION RESULTS

We used a simplified ensemble Monte Carlo model to simulate the transport of a two-dimensional electron gas across a two-dimensional non-planar potential barrier. We included the random inelastic scattering in the Monte Carlo method which reassigns a random momentum to the scattered particle according to Fermi-Dirac statistics. In this way, the electron temperature was kept the same as the lattice temperature at the operation condition. The electron scattering was modeled with a constant relaxation time 88.5 fs for InGaAs material and the estimated electron mean-free-path was 0.188  $\mu\text{m}$  for Fermi energy 526 meV. Since the mean-free-path is small at high doping densities and the electron wave generally loses coherence in the barrier, quantum mechanical interference effects are neglected. The simulation focuses on the effects of non-planar barrier; thus, a constant barrier height of 500 meV was used, rather than a self-consistent band bending calculation that takes into account charge transfers in the structure. This will not change the results significantly because the emitter is much bigger than the interface region and energy distribution of electrons are mostly determined by the bulk emitter. A constant time step of 2 fs was used, which is much less than the scattering relaxation time. The carrier distribution at the quasi-equilibrium state is shown in Fig. 2 (a). The zigzag interface can be clearly seen. Fig. 2 (b) shows the energy distribution of the electrons along the structure. The hot electron filtering of the barrier structure can be clearly seen.

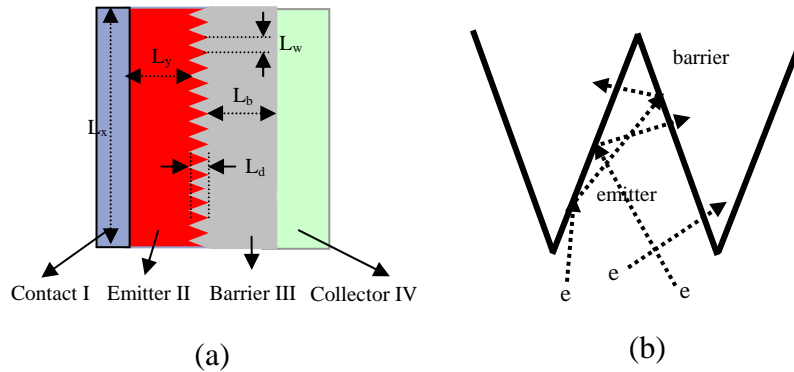


**Fig. 1.** (a) A solid-state thermionic device with non-planar potential barrier, (b) illustration of electron trajectories.

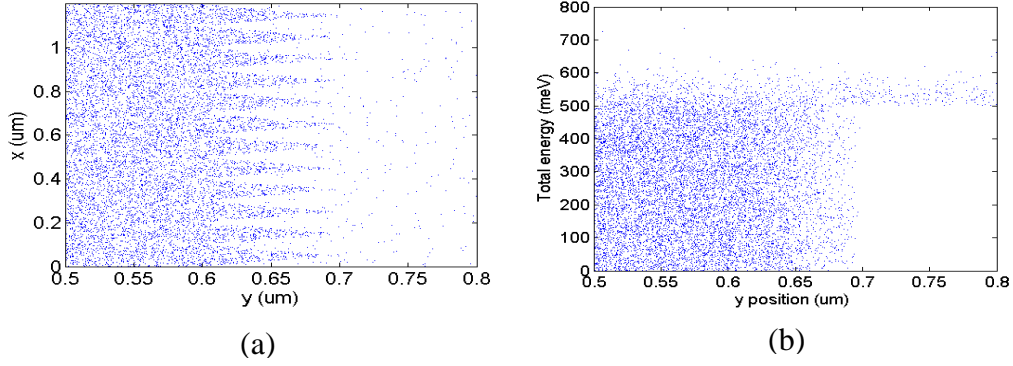


**Fig. 2.** (a) Electron distribution in real space, (b) electron energy distribution along y direction.

Comparing the total currents of the planar and non-planar structures, we can see in Fig. 3 that there is significant enhancement for the zigzag barrier. The width of the planar barrier is assumed to be  $L_b + L_d/2$ . It can be seen that the emitted current increases with the increase of depth  $L_d$  or the decrease of the period  $L_w$ . The dependence on period is easily understood since a larger period is related to a smaller effective interface area and the two regions in the momentum space have larger overlap. These two regions represent emitted electrons with enough kinetic energy perpendicular to each section of the barrier. An increase of the zigzag depth makes the effective interface area larger. However, when period  $L_w$  is small, emitted electrons have more chance to go back to the emitter region for a large zigzag depth. Thus, the improvement converges to an enhancement factor of 1.73 at small periods and large depths.

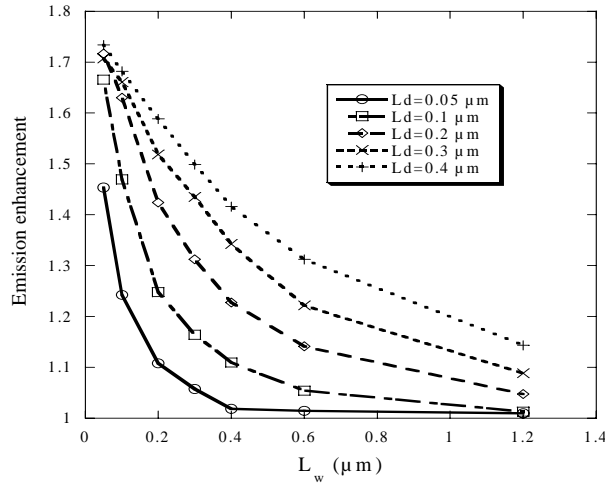


**Fig. 3.** The current enhancement as a function of zigzag parameters.

The chance to have a larger total back-scattering and smaller transmission from a non-planar interface is small. One expects more current emission enhancement from more complex interface geometries. Fig. 4 shows a zigzag interface with four tilted directions. The zigzag period  $L_w$  is divided evenly into four sections; and the zigzag depth is divided to two sections with the ratio of 1:2. The Monte Carlo simulation shows similar dependences on the zigzag period and depth as for the two-direction zigzag case. A factor of 2 improvement in current compared to planar barriers can be achieved for small periods ( $\sim 0.05 \mu\text{m}$ ) and large depths ( $\sim 0.3 \mu\text{m}$ ).

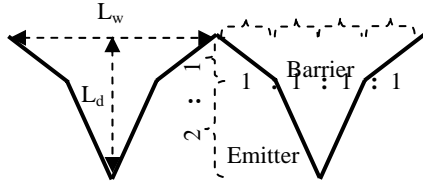


**Fig. 4.** Illustration of the 4-direction zigzagged interface.

One should note that at very small zigzag periods, when the feature size is smaller than the electron de Broglie wavelength ( $\sim 8$  nm), electrons will see an “effective” barrier profile. In this case a more accurate analysis should use 2D Schrodinger equation and calculate the quantum mechanical transmission coefficient. The overall improvement in the number of emitted electrons will persist as long as a larger volume of electrons in the momentum space can participate in the thermionic emission [4].

The Seebeck coefficient of the thermionic heterostructure is proportional to the difference of the average energy of emitted electrons and the Fermi energy. The simulation showed that the Seebeck coefficient depends on the reduced Fermi energy of the barrier  $(E_f - E_b)/k_B T$  very much. The simulation results are plotted in Fig. 5(a) for a 4-direction zigzag with a period of  $0.1 \mu\text{m}$ , a depth of  $0.1 \mu\text{m}$ , and a barrier height of  $500 \text{ meV}$ . It can be seen that the ratio of the Seebeck coefficients of the non-planar barrier and its planar counterpart decreases with the increase of the reduced Fermi energy. However, we can see that electrical conductivity enhancement is more significant in the whole range. As seen in Fig. 5(b) the total thermoelectric power factor ( $S^2\sigma$ ) of non-planar barrier is higher than that of the planar one. It is also shown that the power factor enhancement decreases with the increase of the reduced Fermi energy in the range of interest.

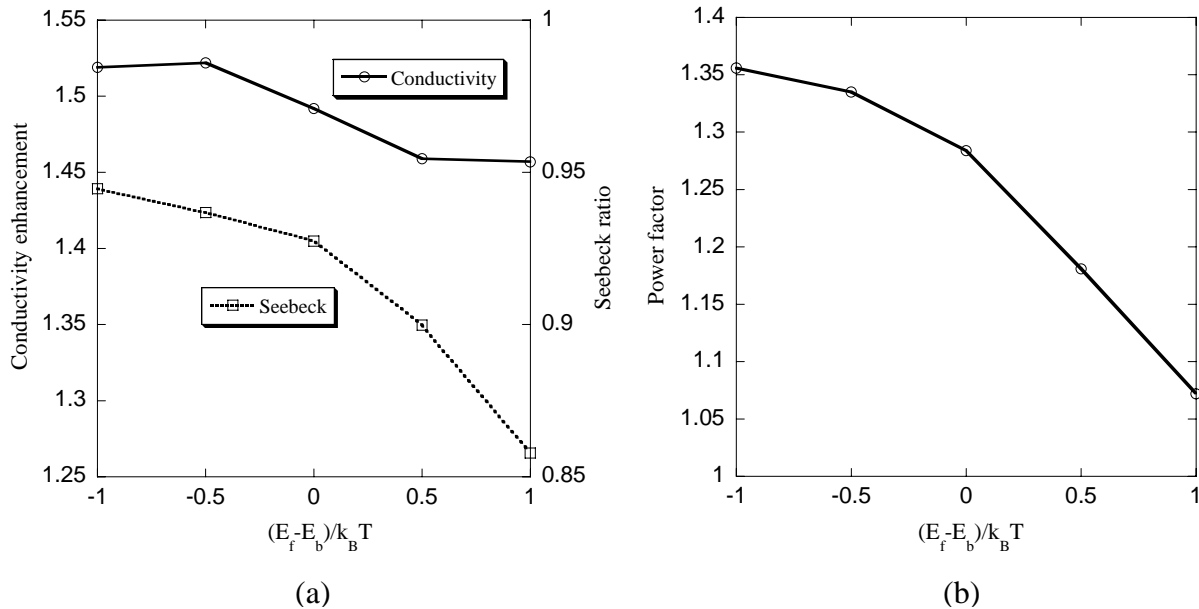


**Fig. 5.** (a) The ratios of the electrical conductivities and Seebeck coefficients of the non-planar barrier and its planar counterpart and (b) the power factor ( $S^2\sigma$ ) enhancement, as functions of the reduced Fermi energy of the barrier.

## HETEROSTRUCTURES WITH EFFECTIVE MASS DIFFERENCE

The fact that electron kinetic energy parallel to an interface could be coupled to the kinetic energy perpendicular to the interface has been overlooked in earlier analysis of heterostructures for thermionic energy conversion. This can happen when electron effective masses are different on the two sides of the interface, which is actually quite common. When an electron passes from a lower effective mass emitter and enters a higher effective mass planar barrier, since both the lateral momentum and total energy is conserved, part of the lateral energy is coupled to the vertical direction and the electron gains momentum in the direction of transport. This kind of electron refraction at hetero interfaces was investigated for the cases of ballistic electron-emission microscopy [11], and resonant tunneling diodes [12]. Grinberg used this theory to solve the puzzle which mass should be used in the Richardson formula for thermionic emission across an interface when there is effective electron mass discontinuity [13]. From the view of wave vector space, the effective volume containing emitted electrons is enlarged and lateral-vertical energy coupling has a similar effect as the lateral momentum nonconservation discussed in Ref. 7.

In Fig. 6, we compared the electrical conductivity of a HgCdTe heterostructure for three different models: (a) no energy coupling between vertical and lateral directions, (b) energy coupling between vertical and lateral directions is determined by the effective masses of the emitter and the barrier, and (c) all the energy at the lateral direction is coupled to the vertical direction. The parameters used in the calculation are similar to those in Ref. 7. Here, barrier width is assumed to be 10 nm, barrier height is 730 meV, effective mass of the emitter is  $0.012 m_e$ , and that of the barrier is  $0.069 m_e$ .  $m_e$  is the mass of a free electron. It can be seen that with large difference of effective masses of the emitter and the barrier, the energy coupling from lateral direction to the vertical direction in model (b) greatly improve the electrical conductivity of the heterostructure compared to that by model (a). Model (c) is only possible with nanostructured design [7] when there is non-conservation of lateral momentum. The thermoelectric figure of merit  $ZT$  is plotted in Fig. 7. Model (b) has very little degradation on Seebeck coefficient and its maximum  $ZT$  has an improvement of above 5 compared to model (a). One should note that if electron effective mass in the barrier is large, electrons will usually have lower mobilities. Thus one has to use thinner barriers to avoid significant scatterings which can reduce the current flow. This can be done as long as cold electron tunneling can be neglected and barrier acts as a good energy filter.

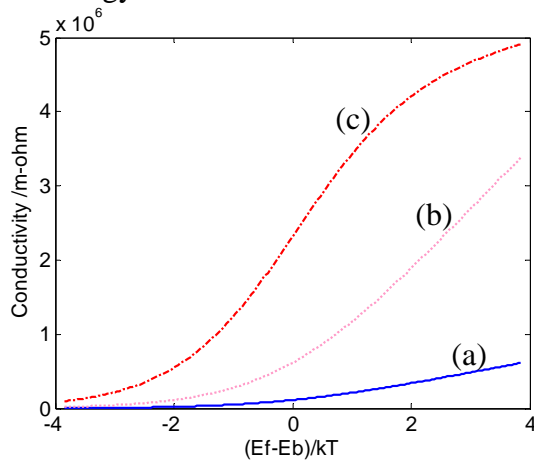


**Fig. 6.** Electrical conductivities of a solid-state thermionic heterostructures for three models.

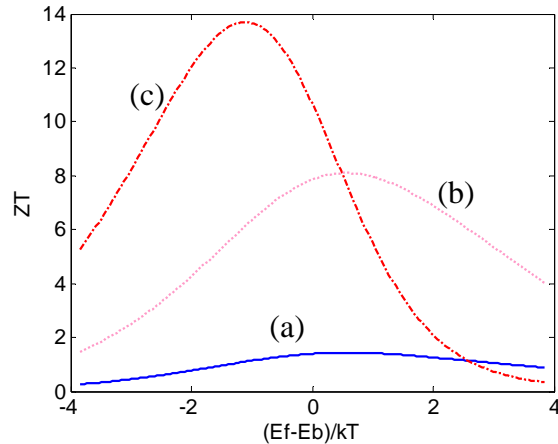


**Fig. 7.** Thermoelectric figure of merit versus reduced Fermi energy for three models.

## CONCLUSIONS

It has been shown that the thermionic emission and electrical conductivity of a heterostructure can be improved by using a non-planar barrier or a planar barrier with a larger electron effective mass than the emitter. The thermoelectric power factor is also increased with the proposed designs. The combined effects of non-planar barrier with a larger effective mass may further improve the thermoelectric properties.

## ACKNOWLEDGEMENTS

This work is supported by the Office of Naval Research (ONR) - Multidisciplinary University Research Initiative (MURI) Grant: Thermionic Energy Conversion Center.

## REFERENCES

1. G. S. Nolas, J. Sharp, and H. J. Goldsmid. *Thermoelectrics: Basic Principles and New Materials Developments* (Springer, Berlin, 2001).
2. A. Shakouri, and J. Bowers, *Appl. Phys. Lett.* **71**, 1234 (1997).
3. G. D. Mahan, and L. M. Woods, *Phys. Rev. Lett.* **80**, 4016 (1998).
4. M. D. Ulrich, P. A. Barnes, and C. B. Vining, *J. Appl. Phys.* **90**, 1625 (2001).
5. G. Chen, and A. Shakouri, *Transactions of the ASME. Journal of Heat Transfer*, **124**, 242 (2002).
6. S. T. Huxtable, A. R. Abramson, C. L. Tien, A. Majumder, C. Labounty, X. Fan, G. Zeng, J. E. Bowers, A. Shakouri, and E. T. Croke, *Appl. Phys. Lett.* **80**, 1737 (2002).
7. D. Vashaee, and A. Shakouri, *Phys. Rev. Lett.* **92**, 106103 (2004).
8. D. L. Smith, E. Y. Lee, and V. Narayanamurti, *Phys. Rev. Lett.* **80**, 2433 (1998).
9. M. Kozhevnikov, V. Narayanamurti, C. Zheng, Y. J. Chiu, and D. L. Smith, *Phys. Rev. Lett.* **82**, 3677 (1999).
10. F. Schubert. *Ligh-Emitting Diodes* (Cambridge University Press, Cambridge, 2003).
11. J. Smoliner, R. Heer, C. Eder, and G. Strasser, *Physical Review B*, **58**, R7516 (1998).
12. Kyoung-Youm Kim, and ByoungHo Lee, *J. Appl. Phys.*, **85**, 7252 (1999).
13. Anatoly A. Grinberg, and Serge Luryi, *IEEE Trans. Electron Devices*, **45**, 1561 (1998).